

A DLS Setup for In-Situ Measurements of Photo-Induced Size Changes of Microgel-based Hybrid Particles

Maren Lehmann,[†] Weronika Tabaka,[†] Tim Möller,[†] Alex Oppermann,[‡] Dominik Wöll,[‡] Dmitry Volodkin,[¶] Stefan Wellert,[†] and Regine von Klitzing^{*,†,§,||}

[†]*Institute of Chemistry, TU Berlin, Berlin, Germany*

[‡]*Institute of Physical Chemistry II, RWTH Aachen University, Aachen, Germany*

[¶]*School of Science and Technology, Nottingham Trent University, Nottingham, United Kingdom*

[§]*Joint Laboratory for Structural Research (JLSR), IRIS Adlershof, HU Berlin, Berlin, Germany*

^{||}*Department of Physics, TU Darmstadt, Darmstadt, Germany*

E-mail: klitzing@fkp.tu-darmstadt.de

Abstract

Photo-induced size changes in microgel particles loaded with gold nanoparticles (AuNPs) were investigated with an extended multi-angle dynamic light scattering (DLS) setup. The DLS setup was equipped with a conventional laser ($\lambda=633$ nm) to determine the microgel particle size. Additionally, a laser ($\lambda=532$ nm) is installed to study the photo-responsive behavior of the AuNP microgel hybrids. The wavelength of 532 nm is close to the absorption maximum of the plasmon resonance of the AuNPs used in the present study (*i.e.* spherical AuNPs with a diameter of 14 nm). The extended

DLS setup enables to follow *in-situ* the change in microgel size during irradiation. The light stimulus is directly correlated with size changes of the hybrid particles and the photo-thermal effect depends on the intensity of the excitation laser. The increase in excitation laser intensity results in a size reduction of hybrid particles due to the ability of AuNPs to partially transform the absorbed photon energy into heat which is emitted into the surrounding microgel network.

Introduction

The ability of photo-responsive polymers to react to light of certain wavelength and change their physical properties very locally is of particular importance in various applications like optical sensors,¹ photo-patterning,² drug delivery³ or cancer treatment.⁴ Photo-responsive polymers often consist of a polymeric matrix combined with a light-sensitive unit creating hybrid particles. The light stimulus triggers a response of the photo-sensitive compound resulting in a reaction of the polymer matrix. Often, dyes⁵ or metal nanoparticles such as silver⁶ or gold nanoparticles⁷ are used as photo-sensitive compounds. Upon irradiation by light with the wavelength of the plasmon absorption the nanoparticle or dye emits heat. If the metal nanoparticles are embedded within a temperature sensitive polymer particle, it can change its size. That means, radiation energy can be transferred to mechanical energy. A popular matrix material for thermoresponsive polymers is poly(N-isopropylacrylamide) (PNIPAM). PNIPAM microgels belong to the class of so-called smart materials since they show a volume phase transition (VPT) induced by external stimuli. Depending on the type of additive (comonomer or nanoparticles) the stimulus can be pH,⁸⁻¹⁰ ionic strength,^{11,12} solvent,¹³ magnetic field,¹⁴ temperature¹⁵ or light.¹⁶ Due to the lower critical solution temperature (LCST) of the monomer NIPAM in water at around 32°C, PNIPAM undergoes a VPT at the same temperature.¹⁵ The VPT is characterized by a rapid and reversible change in the microgel volume.

Photo-responsive hybrid materials, which consist of a photo-sensitive unit emitting heat upon

light irradiation causing a reaction in the thermoresponsive microgel, exhibit the so-called photo-thermal effect.¹⁷

The incorporation of photo-sensitive units into the polymer matrix can be accomplished via various approaches such as the covalent bonding of a dye molecule to the polymer.⁵ Metal nanoparticles can be either synthesized or grown within the polymer network,¹⁸ or prepared separately and later incorporated into the network.¹⁹

In order to quantify the photo-thermal effect, it is necessary to determine the change in the physical properties of the hybrid materials upon irradiation. Nayak *et al.* studied PNIPAM microgels with covalently conjugated malachite green, which is a dye that dissipates heat upon irradiation.⁵ The turbidity of the microgel-dye hybrid suspension was followed while increasing the temperature and compared to the decrease in transmittance upon laser irradiation. The VPT temperature was found to be 31°C for the dye-microgel hybrid. When preheated to 29°C, the reduction in transmittance upon irradiation was similar to the transmittance drop when heated to about 32°C. The change in volume of P(NIPAM-MA) microgel particles loaded with gold nanorods (AuNRs) depending on the laser power was studied by Das *et al.*²⁰ The photo-thermally triggered size changes of the microgels with and without AuNRs were studied at a single detection angle using a PCS setup, which was extended by an excitation laser. The hybrid suspension was preheated to 36°C prior to irradiation, which is close to the VPT temperature of P(NIPAM-MA), that is 38°C. The excitation of the AuNRs leads to a volume decrease in the hybrid particles by 78%, which would equal a temperature increase of 4°C when heated externally. Das *et al.* also noticed a volume change by 25% when irradiating the microgel solution without AuNRs.

Despite light transmission or scattering measurements also optical techniques were employed to study photo-thermal heating. Skirtach *et al.* used the temperature-sensitive dye BCECEF to correlate the fluorescent intensity changes to the temperature developed in the vicinity of polyelectrolyte multilayer capsules containing gold sulfide core/ gold shell nanoparticles during laser irradiation.²¹ Another optical method to detect light-absorbing nanoparticles is

the photothermal interference contrast (PIC) technique,²² where the change in the local index of refraction upon temperature change is detected by the combination of high-frequency modulation and polarization interference contrast by applying a second laser beam.

In order to study the impact of photo-thermal heating, one has to assess the photo-thermal effect at room temperature. The overall goal is to induce the volume phase transition via photo-thermal heating.

In this work, spherical AuNPs are incorporated into PNIPAM microgels and the photo-thermal effect is investigated using an extended DLS setup, where the particle size is determined by HeNe laser irradiation (633 nm) and the additional Sapphire SF 532 laser (532 nm) is used to irradiate the AuNPs in the surface plasmon resonance (SPR) wavelength range. The additional laser (532 nm) combines the advantages of a suitable wavelength to excite the AuNPs and the low absorbance of light by the pure microgel (figure 3(a)). The two-laser DLS setup offers new options to study the hybrid particles at various temperatures, scattering angles and excitation laser intensities. In the case of monodisperse spherical matrix particles in the size range from a few nanometer to several hundreds of nanometer, DLS is a powerful tool to assess the size and its changes upon external stimuli like temperature, whereas in the dispersion of two different scatterers (AuNPs and microgels) not only a purely translational diffusion is probed. For quantitative analysis, a multi-angle DLS setup is required.

Material and Methods

Materials

All materials were used without further purification. For the microgel synthesis, the following chemicals were used: the monomer N-isopropylacrylamide (NIPAM) from Sigma-Aldrich (Germany, purity 99%), cross-linker N,N'-methylenebisacrylamide (BIS) from Fluka (Germany, purity 99.5%) and the initiator 2,2'-azobis(2-methylpropionamidine) dihydrochloride (AAPH) from Sigma-Adrich (Germany, purity 97%). For the synthesis of the gold nanoparti-

cles, sodium citrate dihydrate (purity $\geq 99\%$, Fluka, Germany) and gold(III) chloride hydrate (HAuCl_4 , purity $\geq 49\%$, Fluka, Germany) were used. A three-stage Millipore Milli-Q Plus 185 purification system was used for water purification.

Synthesis of PNIPAM microgel particles

Microgel particles with a cross-linker concentration of 1.25 mol% were synthesized by a surfactant-free precipitation polymerization as described elsewhere.¹⁵ NIPAM (110 mM) and BIS (1.4 mM) were dissolved in 100 mL of water in a batch reactor equipped with an overhead stirrer. After heating up the solution to 80°C and degassing for 30 min, the polymerization was initiated with the addition of 80 mM AAPH dissolved in 1 mL water. After 1.5 hours of reaction, the temperature was quickly decreased to room temperature and the crude microgel particles were purified by dialysing for two weeks against water with daily water exchange. Finally, the microgel was freeze-dried at -85°C and 10^{-3} bar for 72 hours. The PNIPAM microgel particles were found to have a hydrodynamic radius of 298 ± 3 nm at 20°C, which was determined from DLS measurements (LS Spectrometer, LS Instruments AG, Fribourg, Switzerland).

Synthesis of AuNPs

The AuNPs were synthesized according to the method described by Enüstün and Turkevich.²³ All glassware was cleaned by aqua regia before the synthesis. 10 mL of a hot citrate solution (1 wt%) was added to 200 mL of a boiling gold salt solution (5×10^{-4} M HAuCl_4) under vigorous stirring. The growth of the AuNPs was continued for 17 min and afterwards let cool down to room temperature while continuously stirring. The AuNP suspension was used as synthesized without any further purification or dilution **in order to keep the citrate ion concentration constant and to maintain the colloidal stability of the citrate coated AuNP**. The diameter of the AuNP was determined to be 13.7 ± 3.3 nm from transmission electron microscopy (TEM) images. The plasmon resonance wavelength was determined from a UV-

vis spectrum (Varian Cary 50 UV-Vis Spectrophotometer, Varian Medical Systems, Inc., Palo Alto, CA, USA) obtained at 20°C. The concentration of AuNPs after the synthesis was calculated according to the calculations of Haiss *et al.*²⁴ They found that the ratio of absorbance at 450 nm (A_{450}) for the standard path length of 1 cm (d) and the respective molar decadic absorption coefficient (ε_{450} in $M^{-1}nm^{-1}$) gives the concentration (c in $\frac{mol}{L}$) of uncoated spherical AuNPs in water:

$$c = \frac{A_{450}}{\varepsilon_{450} \cdot d} \quad (1)$$

According to that calculation, the aforementioned synthesis led to an AuNP concentration of 7.58×10^{-9} mol L^{-1} . The AuNP suspension was used to prepare the hybrid particles without any further treatment.

Loading PNIPAM microgel particles with AuNPs

In order to prevent aggregation of AuNP within the microgel particles, the AuNP suspension was added to the microgel solution. The PNIPAM microgel solution (0.5 mg mL^{-1}) was mixed with the AuNP suspension in a 1:1 volume ratio. The mixture was shaken for 10 min using a vortex mixer (1000 rpm) and centrifuged for 4 min (8000 rpm). The obtained residue was redispersed in 4 mL water. The washing cycles were repeated till the supernatant was clear. The amount of incorporated AuNPs per one microgel particle was counted from TEM images. The zeta potential was measured with a Zetasizer NanoZS ($\lambda=633$ nm, 4 mW, Malvern Instruments Ltd, Malvern, UK) and were carried out at 20°C. The zeta potential of the microgel (0.1 mg mL^{-1}) was found to be 3.6 ± 0.2 mV. A negative value of -34.4 ± 0.4 mV was measured for the as-synthesized AuNP dispersion, whereas the AuNP-microgel hybrid particles had a zeta potential of -8.7 ± 0.5 mV.

TEM

TEM specimens were prepared via drop coating the TEM grid (copper grid with carbon support film, 200 mesh, Science Services, Munich, Germany) using 5 μL of a sample dispersion. The grids were glow discharged before the coating and blotted with a filter paper after 1 min of the sample application to remove the excess of liquid. The specimen were inserted into the sample holder EM21010 (JEOL GmbH, Eching, Germany) and transferred to TEM (JEOL JEM 2100, JEOL GmbH, Eching, Germany), which was operated at an acceleration voltage of 200 kV. The images were recorded with a bottom-mounted 4k \times 4k CMOS camera system (TemCam-F416, TVIPS, Gauting, Germany) and processed with a digital imaging processing system (EM-Menu4.0, TVIPS, Gauting, Germany). The final image analysis was performed using the software ImageJ (Version 1.46r, Wayne Rasband, National Institutes of Health, USA).

Radial distribution

For the analysis of the radial 3D distributions of AuNPs within the microgels, the center and radius of each microgel was determined in TEM images using custom Matlab routines. The individual AuNPs inside one microgel were localized and the radial distance from the AuNPs to the microgel center was determined. To eliminate the influence of microgel size polydispersity on the distribution analysis, the radial distance was normalized to the corresponding microgel radius. To gain sufficient statistics, the 2D radial distance distributions for 103 microgels were obtained (figure 4(c)) and further analyzed by the software SoMaCoFit²⁵ yielding the average 3D radial distribution of AuNPs inside microgels (figure 4(d)).

Dynamic light scattering setup

The photo-thermally induced size change of the hybrid particles was measured in the DLS mode of a LS Spectrometer (LS Instruments AG, Fribourg, Switzerland) with a HeNe laser

at 633 nm (laser 1). Laser 1 is focused by a lens into the cuvette placed in a temperature-controlled refractive index matching bath filled with decaline and the scattered light detected by an avalanche photodiode detector mounted on a goniometer arm. A second laser (laser 2, Sapphire SF 532, Coherent Inc., Santa Clara, USA) was installed in the conventional setup and focused into the cuvette. Laser 2 is used for photo-thermal heating the hybrid particles and has a wavelength of 532 nm in order to match the plasmon resonance absorption wavelength of the hybrid particles, which exhibits its maximum at around 525 nm at 20°C as determined by UV-vis measurements (figure 3(a)). Whereas the laser 1 used to determine the size of the microgel particles has a wavelength far from the SPR peak of the AuNPs (figure 3(a)). The foci of the excitation laser 2 at 532 nm and of the detection beam at 633 nm overlap in the scattering volume.

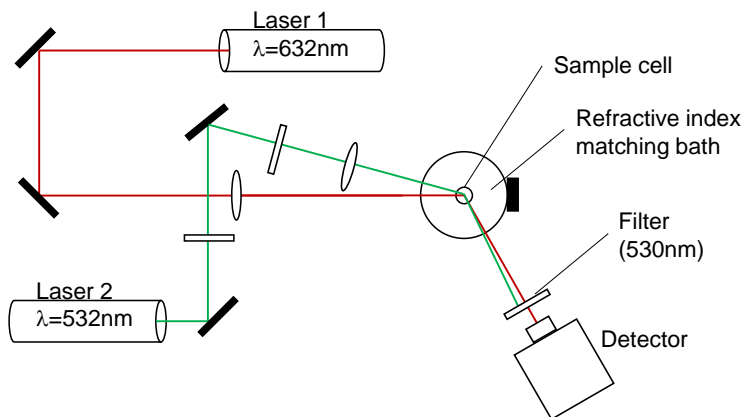


Figure 1: The extended DLS setup with laser 1 ($\lambda=633$ nm) to determine the particles size and laser 2 ($\lambda=532$ nm) to heat the AuNPs in the hybrid particles.

The measured full width at half maximum (FWHM) of laser 2 was 226 μm . It was used to irradiate the AuNPs and was blocked by a filter (OG 530 nm) in front of the detector (figure 1). Hence, detection of scattered green laser light was avoided. Laser 2 was operated at powers (P) between 15 and 150 mW and its intensity (I) was calculated via the laser spot size (A) (equation 2).

$$I = \frac{P}{A} = \frac{P}{\frac{\pi \cdot FWHM^2}{4}} \quad (2)$$

Laser 2 was operated at intensities between 0.3 and 3.2 W/mm². The photo-thermal experiments were conducted at a constant temperature of 20°C in the decaline bath. The scattered light was detected at angles between 30° and 100° with steps of 5° and a duration of 45 sec per each measurement. The multi-angle detection of the scattered light was necessary due to the deviation of the inverse relaxation time divided by the squared scattering vector (Γ/q^2) from the linear fit (figure 2). During the evaluation process, the data resulting in high deviations from the fit were excluded starting at $q=0.13 \text{ nm}^{-1}$ ($=60^\circ$). The obtained raw data were analyzed with a 3rd order cumulant fit in a program written in Python programming language (Python Software Foundation, version 2.7). In the same setup, the deswelling curves of the microgel and the hybrid particles were measured. Therefore, the bath temperature was increased from 20°C to 45°C and the scattered light was detected as described before.

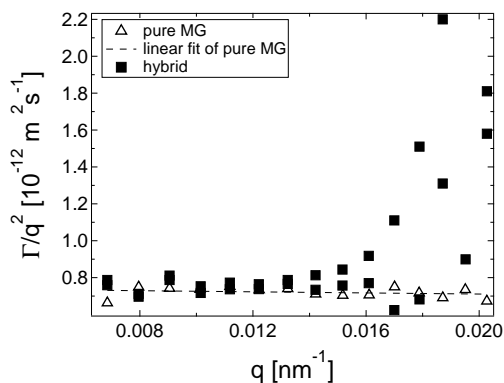


Figure 2: Inverse relaxation time divided by the squared scattering vector (Γ/q^2) of the microgels (open triangles) and the hybrid particles (filled squares) at 20°C plotted against the scattering vector (q).

Results and Discussion

The modified DLS setup enables to perform the temperature dependent and photo-thermal measurements in a single setup, hence without changes of sample environment, sample solution or the cuvette of the samples solutions. First, the measurements at laser 2 intensity variation and secondly, temperature dependent experiments were conducted.

The temperature dependent measurements demonstrate the thermoresponsive behavior of the pure microgel particles and show that the thermoresponsivity is preserved inside the AuNP loaded microgel particles (figure 3b).

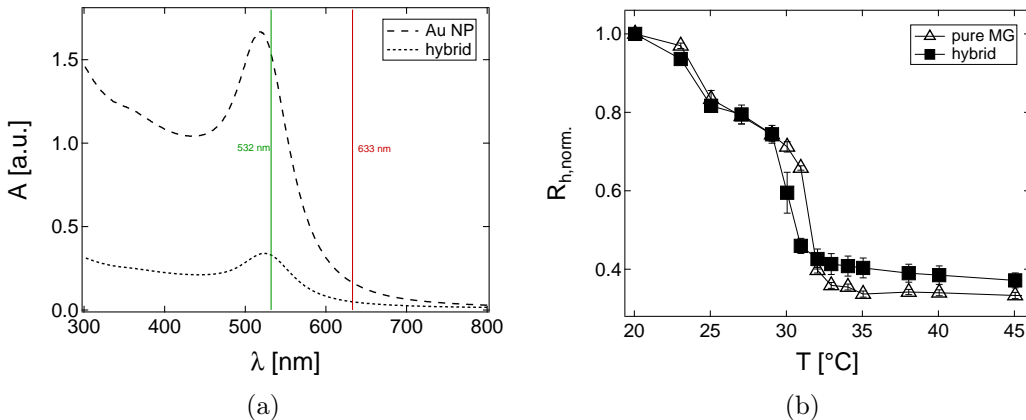


Figure 3: (a) UV-vis spectrum of AuNPs dispersed in water (dashed line) and AuNPs incorporated in microgel particles (dotted line). (b) The relative hydrodynamic radii of the pure microgels (triangles) and the hybrid particles (filled squares) normalized by their size at 20°C as a function of temperature.

The radius of the hybrid particles decreases to 40% upon external heating, which is similar to the microgel particles without AuNPs. Upon decrease of temperature the microgel particles reswell to their original size as well as the hybrid particles, *i.e.* the collapse is reversible. The evaluation of the multi-angle DLS measurements of the hybrid particles reveals the contribution of the AuNPs to the scattered light and the resulting deviation from a linear relationship between Γ/q^2 and the scattering vector (q) (figure 2). A linear relationship between Γ and q^2 is usually expected for translational diffusion of microgel particles. As shown in figure 2, for both systems a constant value of Γ/q^2 was found over the whole

q range in case of the pure microgel, while above $q=0.013 \text{ nm}^{-1}$, the values increase for the hybrid system. Hence, the determination of the hydrodynamic radius is restricted to values below $q=0.013 \text{ nm}^{-1}$. The observed deviations might be due to additional contributions to the diffusion coefficient^{26 27 28} possibly originating from fluctuations of the AuNP within the polymer network.

The mixing of PNIPAM microgel solution and AuNP solution in a 1:1 volume ratio resulted in the formation of AuNP-loaded microgel particles having 74 ± 15 AuNPs per one microgel particle. The TEM images show that the AuNPs are incorporated into the microgel particles (figure 4(a)(b)) which can be attributed to electrostatic attractive interactions between the negatively charged citrate-coated AuNPs and the positively charged microgel.⁷ Due to the low cross-linking density of the microgel particles, the microgel particles have no contrast on the TEM image and only the AuNPs are visible (figure 4(a)(b)). The circular distribution of the AuNPs indicates the size and shape of a single hybrid particle. While the DLS measurements revealed a hydrodynamic diameter of approximately 600 nm for the microgel particles, the TEM images and the AuNP location indicate a diameter of more than 900 nm. This was also found by Gawlitza *et al.* and is explained by the sample preparation for the TEM measurements¹⁹. The adhesion forces between the microgel particles and the carbon support film of the TEM grid cause a flattening and stretching of the particles. The AuNPs in the microgel are well separated and do not form aggregates inside the microgel. The two- and three dimensional AuNP distribution over the radius of one microgel particle was derived from TEM images and shows an increased amount of AuNPs in the outer part of the microgel (figure 4(c)(d)).

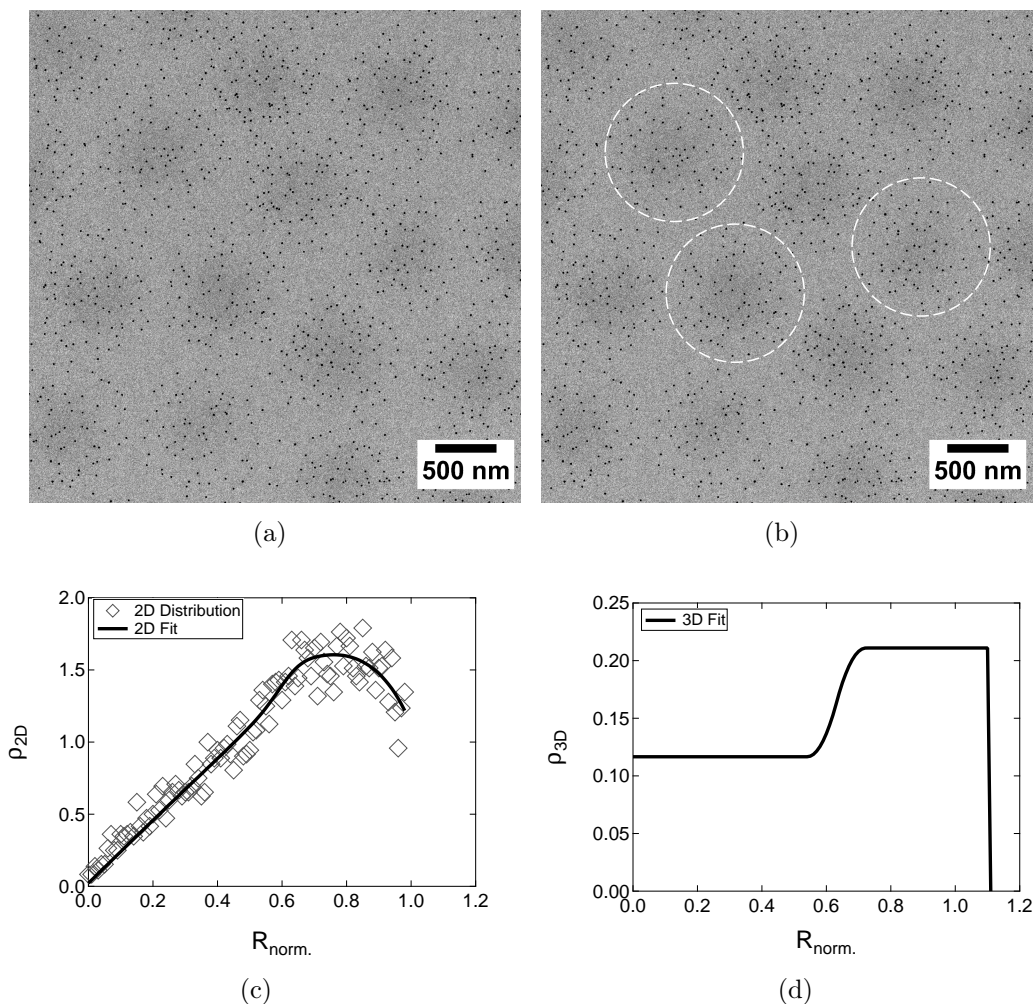


Figure 4: (a) TEM images of hybrid particles; (b) Position of single hybrid particles indicated by white dashed circles. (c) Two-dimensional radial distribution of the AuNPs within the microgel particles. (d) Three dimensional radial distribution of the AuNP positions within the hybrid particles analyzed with SoMaCoFit.²⁵

In order to follow the photo-thermally induced volume changes of the AuNP-microgel hybrids, a solution of them was kept at 20°C in the refractive index matching bath and the intensity of laser 2 was set to 0.3, 1.0, 2.1 and 3.2 W/mm². At each value of the laser 2 intensity, the hybrid solution was irradiated for 5 min before the DLS measurement started. During the detection of the scattered light of laser 1, the laser 2 continuously illuminated the sample. Due to the experimental conditions, all changes in the average hydrodynamic radius of the hybrid particles were attributed to the heat emission at AuNP surface upon laser irradiation.

The pure microgel particles show no response to laser 2 and have a constant hydrodynamic radius throughout the experiments (figure 5(a)). The microgel particles loaded with AuNPs respond to the irradiation by laser 2 resulting in a decrease of the hydrodynamic radius. With increasing intensity of laser 2, the hydrodynamic radius of the hybrids decreases by 17.5% of their initial radius at zero illumination, which would give a volume reduction to 56%. The hydrodynamic radius does not change significantly upon increasing the intensity of laser 2 over 2.1 W/mm² indicating a lower limit in shrinkage upon laser irradiation. In order to verify the reversibility of the size change of the hybrid particle, multiple consecutive cycles of laser 2 on- and off-events were performed as shown in figure 5(b). The hydrodynamic radius of the hybrids decreases to at least 86% of the initial radius and the hybrid particles reswell after switching off laser 2. The repetition of on- and off-laser cycles illustrates the reversible behavior of the hybrid microgels upon the laser irradiation. It points on the ability of the hybrid particles to swell and collapse to their respective relative hydrodynamic radii without showing a hysteresis in the response to the stimulus (figure 5(b)).

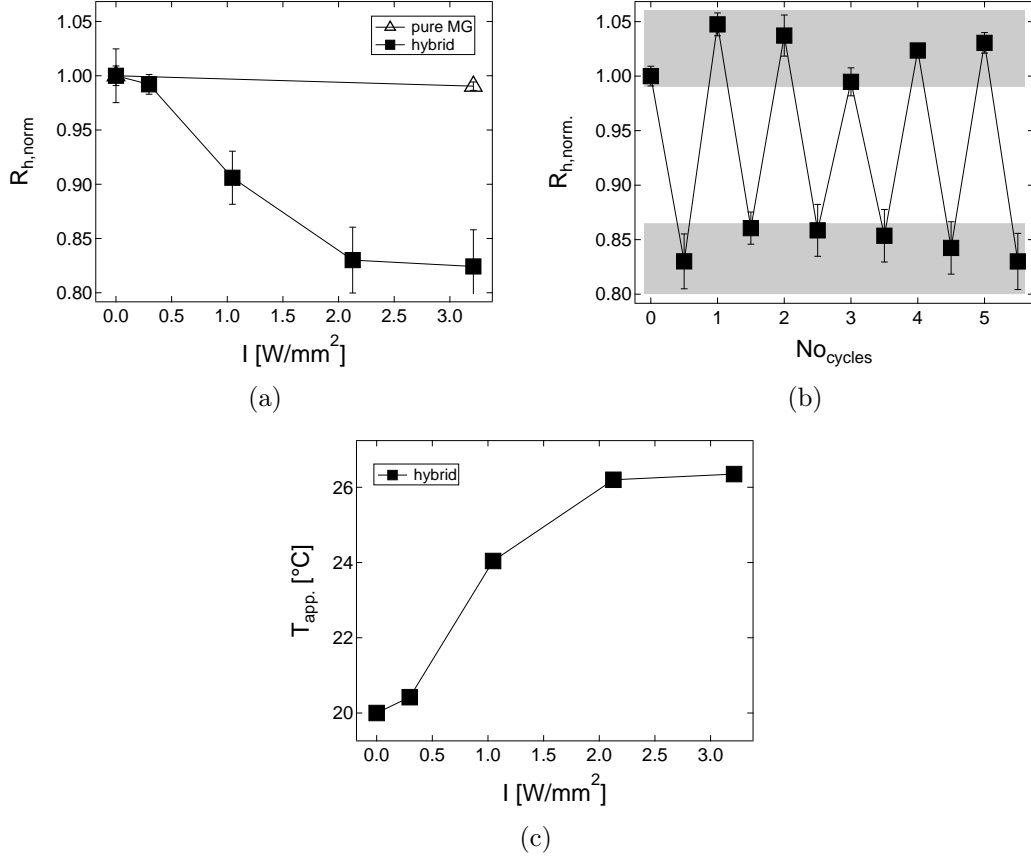


Figure 5: (a) The normalized hydrodynamic radii of the microgel and hybrid particles measured at 20°C as a function of the laser 2 intensity. The particle sizes were normalized to their value at zero illumination. (b) The hydrodynamic radii of the hybrid particles during repeating on/off cycles of laser 2 irradiation starting with an off-event. The hydrodynamic radius is normalized to the radius of the hybrid particle at the beginning of the measurements at at zero illumination. The laser 2 intensity was 2.1 W/mm² at the on-events. (c) The apparent temperature as a function of the laser 2 intensity.

The discrepancy between the minimum radius of 37% of their original radius (*i.e.* 5% in volume ($V_{\text{rel}, \text{collapse}}$)) by external heating and the minimum radius of 83% (*i.e.* 56% in volume ($V_{\text{rel}, \text{total}}$)) by irradiation with the laser 2 might be caused by the inhomogeneous distribution of the AuNPs within the microgel particles. The incorporation in the microgel shell and the short-range heat emission of the AuNPs upon irradiation might cause a collapse only of the shell of the microgel particles and leave the microgel core swollen. This effect would be even more pronounced for gold nanorod- microgel hybrid particles since the AuNRs only cover the microgel particle surface but are not incorporate into the internal volume of

the microgels.^{29,30}

The short-range heat emission was calculated to reach only a few tens of nanometer in the surrounding medium.³¹ Additionally, Govorov *et al.* and Keblinski *et al.* discussed and calculated that the heat generation of a single AuNP leads to a temperature increase of below 10 K depending on the size of the AuNPs. The heat generation of multiple nanoparticles can produce a significant global temperature increase.³²

Assuming a temperature increase at the AuNP surface sufficiently high to fully collapse the surrounding microgel network **and taking into account the heterogeneous radial distribution of AuNP within the microgel (figure 4(d))**, the fraction of microgel volume with incorporated AuNPs can be calculated. At the highest laser intensity (3.1 W/mm²) where the shell of microgel with AuNPs is fully collapsed ($\phi \cdot V_{rel,collapse}$) and the core is still swollen ($(1 - \phi) \cdot V_{rel,swollen}$), the total volume of the hybrid particle ($V_{rel,total}$) can be expressed as follows:

$$V_{rel,total} = \phi \cdot V_{rel,collapse} + (1 - \phi) \cdot V_{rel,swollen} \quad (3)$$

With the assumptions of the total collapse of the shell, the swollen core and the AuNPs being mainly in shell, the volume of the shell can be calculated to be 46% of the total volume of the hybrid particle ($\phi = 0.46$, equation (3), figure 6), which would give a penetration depth of 58 nm.

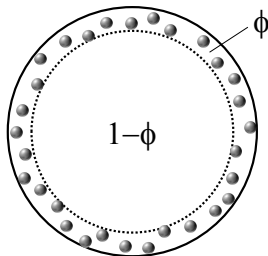


Figure 6: Sketch of the radial distribution of AuNPs within the microgel particle according to the calculation of the shell size.

The result of equation (3) would lead to a hybrid radius fraction of the shell of approxi-

mately 20%, which is supported by the radial 3D distribution (figure 4(d)) considering the flattening and stretching of the hybrid particles upon TEM sample preparation.¹⁹ The heterogeneous distribution of AuNPs within the microgel particle is influenced by the variation of cross-linker density within the microgel particles. The study of the consumption of the cross-linker and the monomer throughout the polymerization indicated a highly cross-linked microgel core and a shell with less cross-linker,^{33,34} which was also shown by small angle neutron scattering experiments³⁵ and atomic force microscopy measurements.³⁶ The radial variation of the mesh size of the microgel network led to the incorporation of the AuNPs in the microgel network only in regions where the distance between two cross-links was large enough for the nanoparticles to permeate through the microgel network.

The apparent temperature (T_{app}) equals the temperature needed by external heating to reach the same relative hydrodynamic radii as for the irradiation with laser 2 and is plotted as a function of the laser 2 intensity in figure 5(c). A relative hydrodynamic radius of 83% of the initial hybrid radius is reached by applying an external temperature of 26°C or a laser intensity of 2.1 W/mm². This single point calibration was done for the entire photo-thermal curve resulting in the plot of figure 5(c). The collapse of the thermoresponsive polymer network can only be caused by a temperature increase, which results from the irradiation of the AuNPs in the photo-thermal experiments.

Nevertheless, the question rises why no stronger heating effect to temperatures beyond the VPT temperature could be observed. Steric hindrance caused by embedded AuNPs can be excluded since temperature depending DLS experiments have shown that above the VPT temperature the hybrid particles collapse to a size similar to the microgel particles without AuNP. The maximum increase in T_{app} is explained by the heterogeneous spatial distribution of the AuNPs within the microgels (figure 4(d)). Furthermore, keeping in mind the distribution of AuNPs in the hybrid particles, the T_{app} (figure 5(c)) does not reflect the temperature rise due to the heat emission of the AuNPs since the T_{app} was averaged over the whole microgel particle and therefore did not take the internal distribution of AuNPs in

the hybrid particles into account.

Conclusion

The multi-angle DLS setup was extended by coupling an additional laser (laser 2) for photo-thermally heating the AuNP-PNIPAM hybrids **enabling the acquirement of absolute values for the hydrodynamic radii and allowing the exclusion of scattered light from the AuNPs during the data evaluation.** In contrast, in a single-angle DLS experiment, the scattered light from the AuNPs would dominate the signal especially at high angles and only relative values for the hydrodynamic radii would be accessible.

][...[The irradiation of AuNPs led to a heat emission into the surrounding microgel network resulting in a size reduction of the overall hybrid particles. Furthermore, the increase of the intensity of laser 2 led to further decrease in the hydrodynamic radius of the hybrids.

][...[According to these averaging considerations **to obtain T_{app} ,** an increases in temperature from 20°C to 26°C could be determined, which is huge in comparison to former studies on photo-thermal heating described in literature and for the first time observed in this temperature regime.][...[

3D analysis of TEM images indicates an incorporation of the AuNPs preferentially in the outer region of the microgel particles. **The heterogeneous spatial distribution of the AuNP within the microgels as well as** the averaging of the size reduction and therefore of T_{app} over the whole hybrid particle led to an underestimation of the temperature reached close to the irradiated AuNPs. However, irradiation cycles (laser 2 on-off) of the hybrid particles showed that the reversibility in the response of the hybrid particle to a stimulus is preserved from the microgel particles without AuNPs.

In order to increase the penetration depth of the AuNPs into the microgel network, homogeneously cross-linked microgels or microgels with functional groups, which interact strongly with the AuNPs might be used. This will give an option to create hybrid particles able

to fully collapse upon irradiation. Furthermore, the extended DLS setup allows to study the size change or destruction of vesicles, microgels or other hybrid systems which have an integrated light-sensitive unit. A wide range of irradiation wavelengths could be adapted to offer a deep investigation of hybrid systems consisting of light-sensitive compounds other than AuNPs, *e.g.* silver nanoparticles, gold nanorods, and others.

Acknowledgement

The authors thank the Deutsche Forschungsgemeinschaft (KL 1165/12-3, VO 1716/2-3) for financial support. A.O. and D.W. acknowledge funding from the Fonds der chemischen Industrie and the collaborative research center SFB 985 of the DFG. The TEM-experiments were carried out at the electron microscope of the Joint Laboratory for Structural Research (JLSR) of Helmholtz-Zentrum Berlin für Materialien und Energie (HZB), Humboldt-Universität zu Berlin (HU) and Technische Universität Berlin (TU). The program to evaluate the data of the DLS measurements was written by Anja Hörmann (TU Berlin) in Python.

References

- (1) Wu, W.; Zhou, S. Hybrid micro-/nanogels for optical sensing and intracellular imaging. *Nano Reviews* **2010**, *1*, 5730.
- (2) Hoffmann, J.; Plotner, M.; Kuckling, D.; Fischer, W.-J. Photopatterning of thermally sensitive hydrogels useful for microactuators. *Sens. Actuators, A* **1999**, *77*, 139 – 144.
- (3) Sershen, S.; Westcott, S.; West, J.; Halas, N. An opto-mechanical nanoshell-polymer composite. *Appl. Phys. B: Lasers Opt.* **2001**, *73*, 379– 381.
- (4) Huang, X.; Jain, P.; El-Sayed, I.; El-Sayed, M. Determination of the Minimum Temperature Required for Selective Photothermal Destruction of Cancer Cells with the Use of Immunotargeted Gold Nanoparticles. *Photochem. Photobiol.* **2006**, *82*, 412–417.

- (5) Nayak, S.; Lyon, L. Photoinduced Phase Transitions in Poly(N -isopropylacrylamide) Microgels. *Chem. Mater.* **2004**, *16*, 2623–2627.
- (6) Skirtach, A.; Antipov, A.; Shchukin, D.; Sukhorukov, G. Remote Activation of Capsules Containing Ag Nanoparticles and IR Dye by Laser Light. *Langmuir* **2004**, *20*, 6988–6992.
- (7) Shi, S.; Wang, Q.; Wang, T.; Ren, S.; Gao, Y.; Wang, N. Thermo-, pH-, and Light-Responsive Poly(N-isopropylacrylamide-co-methacrylic acid)-Au Hybrid Microgels Prepared by the in Situ Reduction Method Based on Au-Thiol Chemistry. *J. Phys. Chem. B* **2014**, *118*, 7177–7186.
- (8) Fernandez-Nieves, A.; Fernandez-Barbero, A.; Vincent, B.; de las Nieves, F. J. Charge Controlled Swelling of Microgel Particles. *Macromolecules* **2000**, *33*, 2114–2118.
- (9) Kratz, K.; Hellweg, T.; Eimer, W. Influence of charge density on the swelling of colloidal poly(N-isopropylacrylamide-co-acrylic acid) microgels. *Colloids Surf., A* **2000**, *170*, 137–149.
- (10) Hoare, T.; Pelton, R. Highly pH and Temperature Responsive Microgels Functionalized with Vinylacetic Acid. *Macromolecules* **2004**, *37*, 2544–2550.
- (11) Karg, M.; Pastoriza-Santos, I.; Rodriguez-Gonzalez, B.; von Klitzing, R.; Wellert, S.; Hellweg, T. Temperature, pH, and Ionic Strength Induced Changes of the Swelling Behavior of PNIPAM-Poly(allylacetic acid) Copolymer Microgels. *Langmuir* **2008**, *24*, 6300–6306.
- (12) Shibayama, M.; Tanaka, T. Volume phase transition and related phenomena of polymer gels. *Adv. Polym. Sci.* **1993**, *109*, 1–62.
- (13) Richter, M.; Zakrevskyy, Y.; Eisele, M.; Lomadze, N.; Santer, S.; Klitzing, R. v. Effect of

- pH, co-monomer content, and surfactant structure on the swelling behavior of microgel-azobenzene-containing surfactant complex. *Polymer* **2014**, *55*, 6513– 6518.
- (14) Backes, S.; Witt, M. U.; Roeben, E.; Kuhrts, L.; Aleed, S.; Schmidt, A. M.; von Klitzing, R. Loading of PNIPAM Based Microgels with CoFe_2O_4 Nanoparticles and Their Magnetic Response in Bulk and at Surfaces. *J. Phys. Chem.* **2015**, *119*, 12129–12137.
- (15) Pelton, R. Temperature-sensitive aqueous microgels. *Adv. Colloid Interface Sci.* **2000**, *85*, 1–33.
- (16) Gorelikov, I.; Field, L.; Kumacheva, E. Hybrid Microgels Photoresponsive in the Near-Infrared Spectral Range. *J. Am. Chem. Soc.* **2004**, *126*, 15938–15939.
- (17) Sershen, S.; Westcott, S.; Halas, N.; West, J. Temperature-sensitive polymer-nanoshell composites for photothermally modulated drug delivery. *J. Biomed. Mater. Res.* **2000**, *51*, 293–298.
- (18) Lange, H.; Juarez, B.; Carl, A.; Richter, M.; Bastus, N.; Weller, H.; Thomsen, C.; von Klitzing, R.; Knorr, A. Tunable Plasmon Coupling in Distance-Controlled Gold Nanoparticles. *Langmuir* **2012**, *28*, 8862–8866.
- (19) Gawlitza, K.; Turner, S.; Polzer, F.; Wellert, S.; Karg, M.; Mulvaney, P.; von Klitzing, R. Interaction of gold nanoparticles with thermoresponsive microgels: Influence of the cross-linker density on optical properties. *Phys. Chem. Chem. Phys.* **2013**, *15*, 15623–15631.
- (20) Das, M.; Sanson, N.; Fava, D.; Kumacheva, E. Microgels Loaded with Gold Nanorods: Photothermally Triggered Volume Transitions under Physiological Conditions. *Langmuir* **2007**, *23*, 196–201.

- (21) Skirtach, A.; Dejugnat, C.; Braun, D.; Susha, A.; Rogach, A.; Parak, W.; Möhwald, H.; Sukhorukov, G. The Role of Metal Nanoparticles in Remote Release of Encapsulated Materials. *Nano Lett.* **2005**, *5*, 1371–1377.
- (22) Cognet, L.; Tardin, C.; Boyer, D.; Choquet, D.; Tamarat, P.; Lounis, B. Single metallic nanoparticle imaging for protein detection in cells. *PNAS* **2003**, *100*, 11350–11355.
- (23) Enüstün, B.; Turkevich, J. Coagulation of Colloidal Gold. *J. Am. Chem. Soc.* **1963**, *85*, 3317–3328.
- (24) Haiss, W.; Thanh, N.; Aveyard, J.; Fernig, D. Determination of Size and Concentration of Gold Nanoparticles from UV-Vis Spectra. *Anal. Chem.* **2007**, *79*, 4215–4221.
- (25) Gelissen, A.; Oppermann, A.; Caumanns, T.; Hebbeker, P.; Turnhoff, S.; Eisold, S.; Simon, U.; Lu, Y.; Mayer, J.; Richtering, W.; Walther, A.; Wöll, D. 3D Structures of Responsive Nanocompartmentalized Microgels. *Nano Lett.* **2016**, *16*, 7295–7301.
- (26) Boyko, V.; Richter, S.; Burchard, W.; Arndt, K. Chain Dynamics in Microgels: Poly(N-vinylcaprolactam-co-N-vinylpyrrolidone) Microgels as Examples. *Langmuir* **2007**, *23*, 776–784.
- (27) Wu, C.; Zhou, S. Internal Motions of both Poly(N-isopropylacrylamide) Linear Chains and Spherical Microgel Particles in Water. *Macromolecules* **1996**, *29*, 1574–1578.
- (28) Trappe, V.; Bauer, J.; Weissmüller, M.; Burchard, W. Angular Dependence in Static and Dynamic Light Scattering from Randomly Branched Systems. *Macromolecules* **1997**, *30*, 2365–2372.
- (29) Karg, M.; Pastoriza-Santos, I.; Perez-Juste, J.; Hellweg, T.; Liz-Marzan, L. Nanorod-Coated PNIPAM Microgels: Thermoresponsive Optical Properties. *Small* **2007**, *3*, 1222–1229.

- (30) Karg, M.; Lu, Y.; Carbo-Argibay, E.; Pastoriza-Santos, I.; Perez-Juste, J.; Liz-Marzan, L.; Hellweg, T. Multiresponsive Hybrid Colloids Based on Gold Nanorods and Poly(NIPAM-co-allylacetic acid) Microgels: Temperature- and pH-Tunable Plasmon Resonance. *Langmuir* **2009**, *25*, 3163–3167.
- (31) Govorov, A.; Richardson, H. Generating heat with metal nanoparticles. *Nano Today* **2007**, *2*, 30–38.
- (32) Keblinski, P.; Cahill, D.; Bodapati, A.; Sullivan, C.; Taton, T. Limits of localized heating by electromagnetically excited Nanoparticles. *J. Appl. Phys.* **2006**, *100*, 054305.
- (33) Wu, X.; Pelton, R.; Hamielec, A.; Woods, D.; McPhee, W. The kinetics of poly(N-isopropylacrylamide) microgel latex formation. *Colloid Polym. Sci.* **1994**, *272*, 467–477.
- (34) Acciaro, R.; Gilanyi, T.; Varga, I. Preparation of Monodisperse Poly(N-isopropylacrylamide) Microgel Particles with Homogenous Cross-Link Density Distribution. *Langmuir* **2011**, *27*, 7917–7925.
- (35) Stieger, M.; Richtering, W.; Pedersen, J.; Lindner, P. Small-angle neutron scattering study of structural changes in temperature sensitive microgel colloids. *J. Chem. Phys.* **2004**, *120*, 6197–6206.
- (36) Fernandes, P.; Schmidt, S.; Zeiser, M.; Fery, A.; Hellweg, T. Swelling and mechanical properties of polymer gels with cross-linking gradient. *Soft Matter* **2010**, *6*, 3455–3458.

Graphical TOC Entry

